information from the Seasat scanning multichannel microwave radiometer (SMMR). As none of these was available for this evaluation, an empirical correction, which is a function of brightness temperature itself, was used. The correction values are based on theoretical calculations and a large number of model atmospheres, and they are generally accurate to only about ± 20 percent.

Some of the results of this initial geophysical evaluation are illustrated in a plot (Fig. 2) of the 139-sample VIRR surface temperature estimates versus the NOAA surface field temperatures interpolated at the same pixel locations; the perfect fit line (slope of unity) and the least-squares linear regression line are shown. The linear regression correlation coefficient, $r = 0.84$, and the root-mean-square difference (or standard error of the estimate) of 1.7°K represent excellent agreement in view of the uncertainty in the atmospheric correction and the uncertainty and the smoothness of the NOAA field. The means of the two sets of temperatures were 293.9°K (VIRR) and 293.1°K (NOAA), and the respective standard deviations were 3.21° and 3.2°K.

We estimated the noise level of the IR data by using a sample of 14 successive pixels on four successive scan lines in an area of relatively low thermal gradient. The standard deviation of all 56 sample pixels from the sample mean of 283.35°K is 0.54°K. When this calculation is repeated with the pixel-to-pixel differences (along with each scan line), the mean difference is −0.04°K and the standard deviation is 0.57°K.

E. PAUL MCCLAIN
National Environmental Satellite Service, National Oceanic and Atmospheric Administration, Washington, D.C. 20233
RICHARD A. MARKS
Jet Propulsion Laboratory, California Institute of Technology, Pasadena 91103

Note

1. The research described in this report was carried out by the Jet Propulsion Laboratory, California Institute of Technology, under NASA contract NAS7-100.

20 April 1979

Venus: Further Evidence of Impact Cratering and Tectonic Activity from Radar Observations

Abstract. *Earth-based radar images at a resolution of 10 kilometers show a diverse surface terrain on Venus, probably produced by both impact events and tectonic activity. Only a small number of craters of apparent impact origin are seen. Large-scale features show lineaments and parallel ridges suggesting tectonic origins.*

On 20 June 1972, Rumsey *et al.* (*1*), using the Jet Propulsion Laboratory–NASA (JPL-NASA) planetary radar system, obtained both an image and an altitude map of a small area surrounding the sub-Earth point on Venus for that day. This image, which was at a resolution (*2*) of approximately 10 km, showed what appeared to be a crater 160 km in diameter, the first reasonably unambiguous identification of a small feature on the surface of the planet. Since that time Goldstein *et al.* (*3, 4*), using the JPL-NASA system, have produced images and altitude maps of a number of regions near the equator, while Campbell *et al.* (*5*), using the radar system at the Arecibo Observatory, have produced an image covering a large area at high northern latitudes. These images show a diversified surface. Evident are a number of small and large roughly circular structures, a 1000-km-long trough, numerous isolated peaks, and a number of large irregularly shaped areas of high surface roughness. On the basis of gross morphology and size distribution, Saunders and Malin (*6*) suggested that a group of these circular features in one region may be impact craters while two others may be volcanic constructs. The 1000-km-long trough they interpret in terms of a rift valley. This report presents a number of new images which support the suggestion that the surface of Venus shows a history of both impact events and tectonic activity.

Venus was mapped with the Arecibo 12.5 cm wavelength radar in 1975 and 1977. The 1975 observations were limited to relatively high latitudes and to resolutions larger than 10 km, while the 1977 observations concentrated on the lower latitudes and achieved resolutions down to 5 km over a few regions. Combining the images from the 2 years will give coverage of most of the area between longitudes 270° and 20° and from latitude 60°S to 70°N. A strip from roughly 10°S to 10°N will be either missing or of poor quality.

Figures 1 through 3 are images in a Mercator projection (*7*) covering regions in the vicinity of the first two features discovered on the surface of the planet in 1962 (*8*) and tentatively named Alpha and Beta at that time. For all these images the average scattering properties of the planet have been removed (*9*) so that one sees the ratio between the received power from a particular area and that expected for a homogeneous surface having the same average properties as are observed for Venus. Increasing brightness corresponds to increasing levels of power backscattered toward the radar per unit surface area on the planet. In general, most brightness differences are due either to changes in the average slope of the surface over the resolution cell so that the effective incidence angle (θ) is changed or to differences in the degree of small-scale surface roughness (on the order of the wavelength of the incident radiation). At incidence angles below about 15° the scattering law [see (*9*)] is very sensitive to changes in the average slope. Good examples of this are crater walls, mountainsides, and so on. At angles above 30° most contrast changes appear to be determined by differences in small-scale surface roughness. The greater the roughness, the brighter the reflection. In theory, changes in the dielectric constant of the surface material due to differences in composition, or in compactness for powdered surfaces, should be discernible, but generally these seem to be masked by changes in the surface roughness. At the intermediate angles between about 15° and 30° contrast differences may be due to changes in either the average slope or the small-scale surface roughness, but they tend to be rather small.

Although a number of "craterlike" and "basinlike" formations can be seen in the images, most of the regions of high reflectivity have rather amorphous shapes. This situation is exemplified by the region in the vicinity of the feature Alpha shown in Fig. 1a. The whole southern part of this image is dominated by irregularly shaped areas of rough terrain. Most of them tend to be rather elongated and some are more than 1000 km in extent. It should be emphasized that while the enhancement of the backscattered signal is probably due to an increase in the small-scale roughness, this may be associated with changes in surface roughness on very much larger scales. Alpha is the bright region approximately 1300 km in diameter toward the upper right (east) in Fig. 1a. Just south of Alpha is a circular feature 280 km in diameter with a prominent central bright spot. A group of smaller but otherwise similar features are visible to the west of Alpha. Figure 1b is a higher resolution photograph of this latter region. All of these features have characteristics that suggest impact craters, although topographic information is needed to confirm this interpretation. Of the approximately 16 features of this type that we have found, 70 percent have discernible "central" bright spots. This is in reasonable agreement with the approximately 80 percent of impact craters with central peaks in this size range on Mercury and Mars (*10*).

Immediately to the west of Alpha are what appear to be the remnants of two overlapping roughly circular features, both of which are about 800 km in diameter. It seems to be possible to trace the edge of the southernmost one through the western part of Alpha. A number of these large, roughly circular features with dark, and hence probably smooth, floors have been found. One characteristic of most of them is the presence of a small bright area similar to the central bright spots of the craters of Fig. 1b. Two typical examples can be seen in the features west of Alpha. Again, we have no topographic information on these large circular features in the Arecibo images. Several similar features have been observed by Goldstein *et al.* (*3, 4*) and their altitude measurements suggest that the floors of these features are lower than the surrounding terrain.

Alpha itself is one of the most remarkable areas so far observed on Venus. Two views of it are shown in Fig. 1, a and c. These images were made in 1975 and 1977, respectively, at resolutions of 10 and 5 km, and the incidence angles at which the center of the feature was viewed were 50° and 23°. In Fig. 1c the northwestern part of the feature appears somewhat darker than it should since the average scattering law of the planet has been divided into the data and the areas contained within Alpha follow a much flatter scattering function than the average law. At the larger incidence angles of Fig. 1a the difference in the scattering laws is much smaller. The major features of Alpha are discernible in both images. However, the higher resolution, lower incidence angle image of Fig. 1c shows a large number of approximately parallel lineaments that are not visible in Fig. 1a. Some of these lineaments can be traced for several hundred kilometers and they are separated by approximately 20 km. That they cannot be seen in Fig. 1a is not thought to be due to the lower resolution but rather to the higher incidence angle. If this is so, then we are probably seeing enhancements due to increases in average slope indicating the presence of a series of parallel ridges or valleys. A general herringbone pattern is apparent in the northwest of Alpha in Fig. 1a but it does not seem to bear any relationship to the lineaments of Fig. 1c. The central dark spot visible in Fig. 1a is only barely discernible in Fig. 1c.

We turn now to the images of the Beta region in Fig. 2. Beta is the large bright feature to the left in Fig. 2a and an enhanced version of this part of the same image is shown in Fig. 2b. The general outline of this feature, including the small central dark area, agrees well with the observations of Goldstein *et al.* (*4*) at slightly lower resolution. The major difference between the two observations is the narrow tongues of apparently rough material extending, some for more than 500 km, from the main part of Beta. These are only hinted at in the JPL image. There has been considerable speculation as to whether Beta is of impact or of volcanic-tectonic origin. In addition to their image of Beta, Goldstein *et al.* also measured a height for this feature of 10 km. On the basis of these observations, Saunders and Malin (*6*) interpreted Beta to be a large volcanic construct. The observations reported here tend to favor this interpretation. Although Beta has a

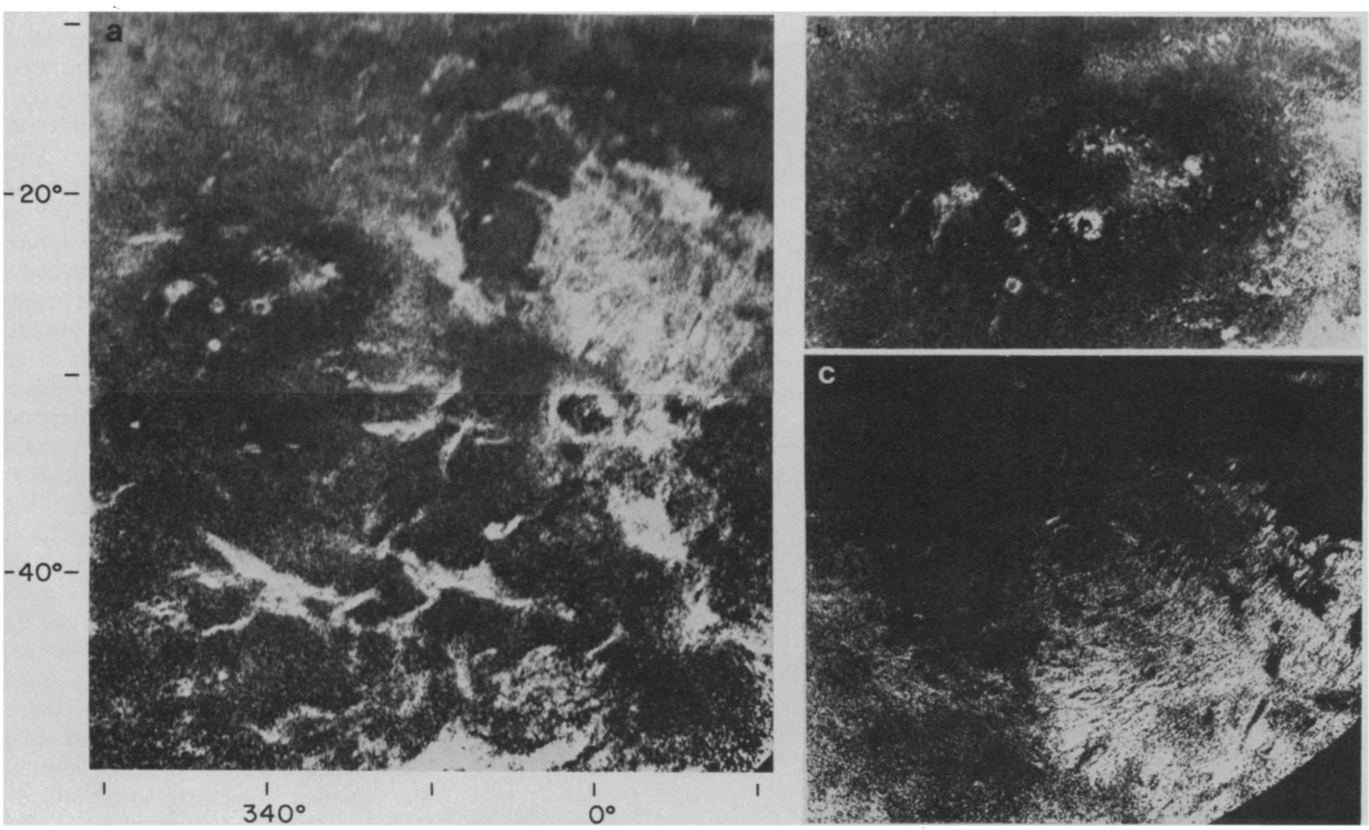

Fig. 1. (a) Alpha and the surrounding region at an average resolution of 10 km. Approximately 100 independent estimates of the power backscattered from each resolution cell (commonly called "looks") from 4 days in early September 1977 were averaged to produce this image. (b and c) Images at 5-km resolution of the group of craters to the upper left in (a) and of Alpha itself; each represents an average of about 30 looks in April 1977. Note the rather asymmetric rough margins and offset "central" bright spots for two of the craters in (b).

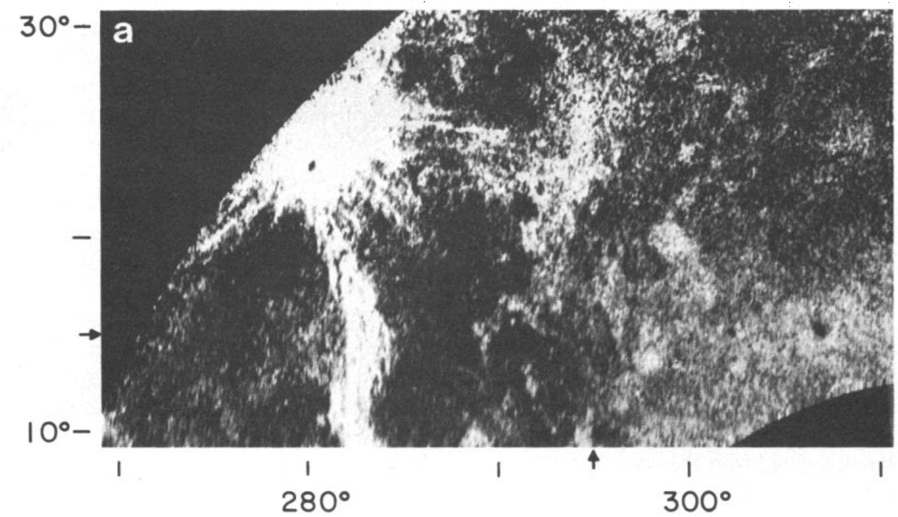

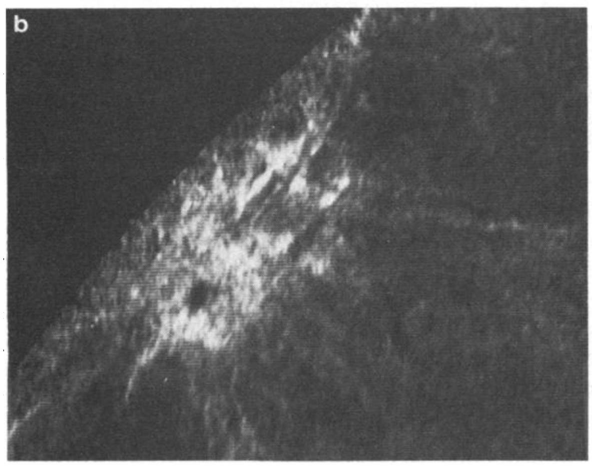

Fig. 2. Beta and the region east of it at an average resolution of 10 km. The image in (b) is an enhanced version of the left side of (a) showing the structure of Beta itself. About 50 "looks" were averaged to construct this image from data from March 1977. The site of the Venera 10 landing is indicated by the two arrows at latitude 15°N and longitude 295°.

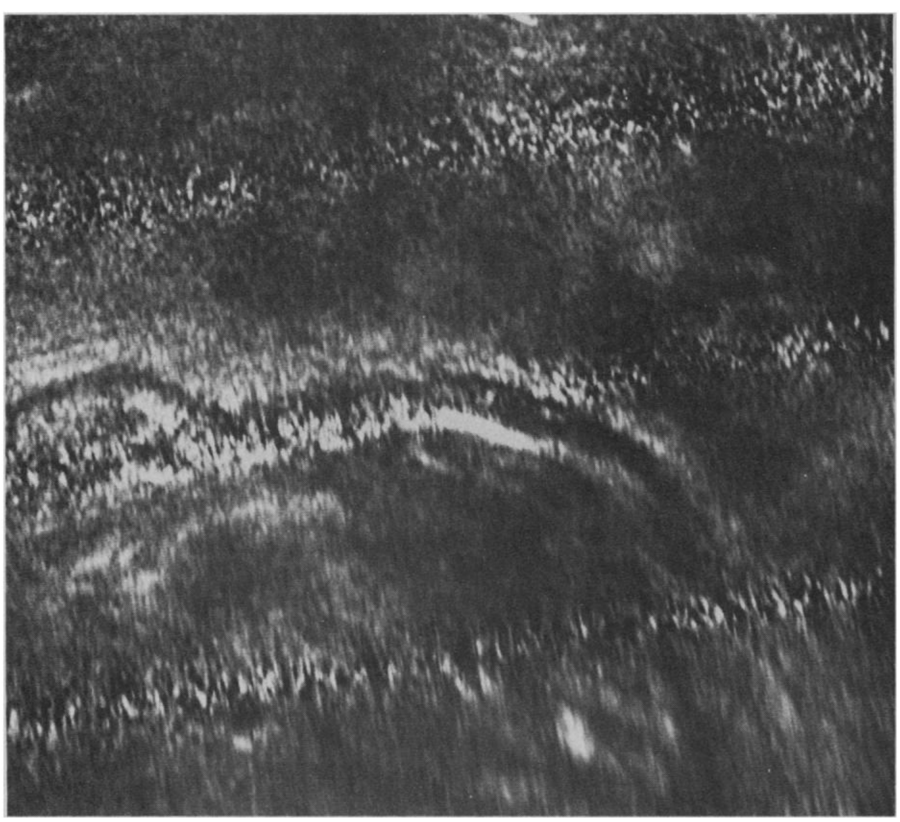

Fig. 3. A 1000-km-long pair of parallel ridges. The area imaged is between latitudes 0° and 11°N and longitudes 349° and 1°. The three equally spaced straight, parallel bands are artifacts of the data acquisition technique.

roughly circular shape, it bears little resemblance to any of the other probable impact craters so far discovered on Venus. If Beta is of volcanic origin, then the "rays" of Fig. 2 may be flows or, perhaps, approximately radial fractures similar to those in the Tharsis region on Mars (*11*). In the latter case the narrow feature extending more than 1000 km south of Beta may be a rift system similar to Valles Marineris. It terminates just to the south of the area in Fig. 2a and does not seem to connect to the large canyon reported by Goldstein *et al.* (*3*), which crosses the equator just to the east.

Indicated on Fig. 2a is the location of the Venera 10 landing site. The image from this lander showed a flat, eroded-looking surface (*12*), which is moderately consistent with the general terrain shown for the region in Fig. 2a. Immediately to the northeast of this landing site is a circular, low-reflecting region 250 km in diameter surrounded on three sides by a large area of higher contrast material, which is very clearly outlined against the surrounding terrain.

One of the more striking features we have discovered is shown in Fig. 3. This image shows two curved parallel ridges extending for more than 1000 km just north of the equator. (The three straight, evenly spaced, almost horizontal bands are artifacts of the fringe pattern of the interferometer used for data acquisition.) We know that these are ridges because of the bright specular echo from the center of the southern ridge and, to a lesser extent, from the northern one. This specular highlight has been observed to move as the planet rotates. The size of the specular echo relative to the return from the surrounding terrain indicates a positive slope of about 6°, which, combined with a measured width of 20 km, gives a height for the southernmost ridge of roughly 2 km. This very approximate calculation is based on the assumption that the scattering law given in (*9*) applies to the terrain in this particular area. The low signal strength between the ridges is probably due to a reverse slope, but the depth of the resultant "valley" cannot be estimated.

It seems probable that we are seeing evidence of both impact events and tectonic processes, although only a small number of possible impact craters have been found and only one area of what could be described as cratered terrain. We should emphasize that highly eroded, relatively smooth surfaced craters may not be very visible at the high incidence angle and relatively low signal-to-noise ratio of most of the Arecibo images. The complete lack of altitude information severely limits our ability to make definitive statements about most of the features in these images. This problem will be at least partly solved by the Pioneer Venus orbiter, which is currently supplying altitudes at approximately 120-km spacings over the region covered by the Arecibo images. The combination of the two data sets should lead to a much better understanding of the nature of the large surface structures visible in the radar images.

D. B. CAMPBELL
B. A. BURNS, V. BORIAKOFF
National Astronomy and Ionosphere Center, Arecibo, Puerto Rico 00612

References and Notes

1. H. C. Rumsey, G. A. Morris, R. R. Green, R. M. Goldstein, *Icarus* **23**, 1 (1974).
2. Traditionally, the resolution of maps from Earth-based radars has been quoted in terms of the width of the ambiguity function of the radar. This resolution is very close to a factor of 2 smaller than the "line pair" resolution normally used by photogeologists, so that 5 km (radar) is 10 km (line pair).
3. R. M. Goldstein, R. R. Green, H. C. Rumsey, *J. Geophys. Res.* **81**, 4801 (1976).
4. ——, *Icarus* **36**, 334 (1978).
5. D. B. Campbell, R. B. Dyce, G. H. Pettengill, *Science* **193**, 1123 (1976).
6. R. S. Saunders and M. C. Malin, *Geophys. Res. Lett.* **4**, 547 (1977); *Geol. Rom.* **15**, 507 (1976).
7. All longitudes used are based on the International Astronomical Union defined values for the prime meridian and rotation period as given in the "Report of Commission 16 of the International Astronomical Union" [*Trans. IAU* **14B**, 128 (1970)]. The position of the north pole used is the same as that adopted by the Pioneer Venus project, which, in 1950.0 coordinates, is: right ascension, 273.3°; declination, 67.3°.
8. R. M. Goldstein, *Radio Sci.* **69D**, 1623 (1965).
9. The average scattering properties for Venus seem to be well represented by Hagfors' one-parameter scattering law [T. Hagfors, *J. Geophys. Res.* **69**, 3739 (1964)]: $\sigma_0(\theta) \propto (\cos^4\theta + C\sin^2\theta)^{-3/2}$, where $\sigma_0(\theta)$ is the specific backscatter cross section per unit area of the surface, θ is the incidence angle of the incoming wave to the surface, and C is a parameter that is essentially determined by the root-mean-square surface slope. A C parameter of 175 was found to give a good fit to the measured average scattering law for $0° \leq \theta \leq 40°$. For values of θ greater than 40°, the scattering law was assumed to behave as $\cos^{1.5}\theta$.
10. M. H. Carr, L. S. Crumpler, J. A. Cutts, R. Greeley, J. E. Guest, H. Masursky, *J. Geophys. Res.* **82**, 4055 (1977).
11. M. H. Carr, *ibid.* **79**, 3943 (1974).
12. M. V. Keldysh, *Icarus* **30**, 605 (1977).
13. We thank R. B. Dyce, A. Crespo, T. Dickinson, A. Hine, R. Olver, R. Payne, R. Velez, and the staff of the Arecibo Observatory for their assistance. We thank D. Elliott and the staff of the Image Processing Laboratory at JPL for converting the images from digital form to photographs and I. Shapiro for supplying the necessary planetary ephemerides. The National Astronomy and Ionosphere Center is operated by Cornell University under contract to the National Science Foundation and with support from the National Aeronautics and Space Administration.

22 March 1979; revised 29 May 1979

Dynamic Changes in Circulating 1,25-Dihydroxyvitamin D During Reproduction in Rats

Abstract. *The concentrations of 1,25-dihydroxyvitamin D [1,25-$(OH)_2D$], calcium, and phosphorus were measured in the serum of rats during pregnancy and at various stages of lactation. The concentration of 1,25-$(OH)_2D$ hormone increased almost twofold during pregnancy and the latter part of lactation, but decreased to control levels or very low values immediately after birth and weaning, respectively. Furthermore, the concentration of 1,25-$(OH)_2D$ was inversely correlated with the concentration of calcium, suggesting that circulating 1,25-$(OH)_2D$ fluctuates in concert with calcium demands during the reproductive cycle. Parathyroidectomy in lactating rats caused a 70 percent inhibition of the normally observed 1,25-$(OH)_2D$ increase, indicating that parathyroid hormone, in response to changes in serum calcium, is a primary modulator of 1,25-$(OH)_2D$ during lactation.*

The mineral requirements of the fetus during pregnancy and the high rates of mineral transfer to milk during lactation impose substantial drains on maternal calcium and phosphorus stores (*1*). These stores are maintained and replenished by increases in intestinal absorption of calcium and phosphate, processes known to be mediated by 1,25-dihydroxyvitamin D [1,25-$(OH)_2D$] (*2*). This active vitamin D metabolite, which also participates in calcium homeostasis, is formed in a tightly controlled fashion in the kidney (*3*) under the influence of a host of regulators including calcium (*4*), phosphate (*5*), parathyroid hormone (PTH) (*5, 6*), growth hormone (*7*), estrogen (*8*), and prolactin (*9*).

Near the end of pregnancy in humans (*10*) and late in lactation in rats (*11*), striking increases are observed in the concentration of 1,25-$(OH)_2D$ in the serum. Little is known about the factors responsible for triggering the increase in circulating 1,25-$(OH)_2D$ during the reproductive period. We therefore conducted experiments in rats to monitor serum 1,25-$(OH)_2D$, calcium, and phosphorus at a number of periods between late pregnancy and the termination of lactation and to determine if, during lactation, the absence of PTH might significantly alter serum 1,25-$(OH)_2D$ and therefore implicate PTH as a major regulating factor.

Female rats (Holtzman) were obtained when they were 6 or 14 days pregnant, when they had litters of ten 7- to 15-day-old pups, or when they were nonlactating adults. All rats arrived in the laboratory 6 days or more before the beginning of the experiment and were maintained on a diet (*11*) consisting of 75 percent whole wheat flour, 13 percent casein, 4.4 percent fat (mostly as corn oil), 2 percent salt mixture, 1.3 percent of vitamin D–free vitamin mixture (ICN Life Sciences), and 0.8 percent $CaCO_3$, with final calcium and phosphorus contents of 0.37 and 0.32 percent, respectively. Vitamin D_3 was added at 5 I.U. per gram of diet.

Calcium, phosphorus, and 1,25-$(OH)_2D$ were determined in the serum of rats at different reproductive stages (six to eight animals per group). The stages used were pregnancy (at 21 days), shortly after birth (1 to 2 days), lactation (7 to 8 days and 13 to 16 days), and postlactation (2 and 7 days after weaning). Nonlactating controls, in which lactation had been terminated 2 weeks or more, were also included. Control rats for individual reproductive groups were killed at times ranging from 6 to 20 days after receipt in the laboratory, corresponding to the time the pregnant and lactating rats were killed. Serum calcium was determined in a lanthanum chloride solution (1 percent lanthanum) by atomic absorption spectrometry with a Perkin-Elmer 305 instrument. Phosphate (as inorganic phosphorus) was determined colorimetrically (*12*). The remaining serum (3 to 5 ml per rat) was frozen (−90°C) for subsequent determinations of 1,25-$(OH)_2D$, which was measured by a radioreceptor assay with the chick intestinal cytosol-chromatin receptor system as originally described by Brumbaugh *et al.* (*13*) and modified as detailed elsewhere (*9*).

Recently, we have used 1,25-$(OH)_2$-$[^3H]D_3$ of very high specific activity (94 Ci/mmole) to increase the sensitivity of the assay to 1 pg of 1,25-$(OH)_2D$ which allows analysis of individual rat serum samples. The 1,25-$(OH)_2D$ was isolated from serum prior to assay either as described by Hughes *et al.* (*14*) or by recent modifications incorporating high-pressure liquid chromatography (*15*). Standard errors were calculated from analysis of variance of the data in each experiment and a one-tailed Student's *t*-test was used to test significance of differences between mean values. Significance of correlation coefficients was tested according to Mack (*16*).

Figure 1 indicates that a significant increase in 1,25-$(OH)_2D$ occurs in late pregnancy in rats, as in humans. This in-

0036-8075/79/0629-1427$00.50/0